Int. J. Dev. Biol. 51: 351-360 (2007)
doi: 10.1387/ijdb.062258sr

Original Article

The retinoic acid metabolising gene, CYP26B1, patterns the cartilaginous cranial neural crest in zebrafish

SUSAN REIJNTJES[1], ADAM RODAWAY[1] and MALCOLM MADEN*[,2]

[1]Randall Division of Cell and Molecular Biophysics and [2]MRC Centre for Developmental Neurobiology, King's College London, UK

ABSTRACT We have investigated the function of the retinoic acid metabolising enzyme, CYP26B1, by administering an antisense morpholino oligonucleotide to zebrafish embryos. The result was an alteration in the morphology of the embryo in those regions which express the gene, namely an embryo with a smaller head, correspondingly smaller hindbrain rhombomeres and severely reduced numbers of vagal brachiomotor neurons. Most strikingly, these embryos had defective or absent jaw cartilages implying a role for this enzyme in patterning or migration of the neural crest cells which give rise to this tissue type. In order to determine whether this phenotype resembles that of excess retinoic acid or a deficiency of retinoic acid, we compared the jaw defects following retinoic acid treatment or DEAB treatment, the latter being an inhibitor of retinoic acid synthesis. The effects of the inhibitor rather than excess retinoic acid most closely phenocopied the jaw defects seen with the *Cyp26B1* morpholino which suggests that, at least in the zebrafish embryo, the action of CYP26B1 in the neural crest may not be simply to catabolise all-*trans*-RA.

KEY WORDS: *Cyp26B1, zebrafish, morpholino, neural crest, retinoic acid, RA, jaw cartilage*

Introduction

Signalling systems in the developing embryo routinely rely on negative feedback control to switch off the inductive signal once it has performed its task on neighbouring cells (Freeman, 2000). Examples of this phenomenon include sprouty/FGF, noggin/BMP, Dkk/Wnt and in the case of the retinoic acid (RA) signalling pathway, enzymes of the P450 class, the CYP26s, are thought to be responsible for switching off the RA signal. RA is synthesised in cells from its precursor, retinol, by the retinaldehyde dehydrogenases (RALDHs) and it signals to adjacent cells in a paracrine fashion (review, Maden 2002) by entering the nucleus of responding cells to induce a novel pattern of gene expression. This is performed by binding to the retinoic acid receptors (RARs) and the retinoid X receptors (RXRs) which are ligand activated transcription factors (Kastner *et al.,* 1994; Kliewer *et al.,* 1994). There are 3 *Cyp26* genes, *Cyp26A1*, *Cyp26B1* and *Cyp26C1* and each metabolises all-*trans*-RA into more polar compounds such as 4-*oxo*-RA, 18-OH-RA, 4-OH-RA and 5,6-*epoxy*-RA (Fujii *et al.,* 1997; White *et al.,* 1997; White *et al.,* 2000). They show dynamic and non-overlapping distributions in the developing mouse, chick, *Xenopus* and zebrafish embryo (Fujii *et al.,* 1997; de Roos *et al.,* 1999; Swindell *et al.,* 1999; MacLean *et al.,* 2001; Reijntjes *et al.,* 2003; Reijntjes *et al.,* 2004; Tahayato *et al.,* 2003; Emoto *et al.,* 2005; Zhao *et al.,* 2005; Gu *et al.,* 2005).

Thus within a developing field of cells where RA is required for patterning, one of the RALDHs should be present in signalling cells and one of the CYP26s should be present in cells which function as a sink, thereby generating a gradient of RA between them. Such a system may operate to pattern the posterior hindbrain within the neural plate where *Raldh2* is present in the underlying mesenchyme posterior to the level of the first somite and *Cyp26C1* is present in the anterior mesenchyme (Reijntjes *et al.,* 2004). There is a gap in between these two expression domains within which a gradient of RA could be generated permitting patterning of the overlying posterior hindbrain. A further model of hindbrain patterning encompasses the differing expression domains of *Cyp26A1* and *C1* and envisages their function as sequential barriers limiting the anterior spread of RA signalling through the hindbrain rhombomeres (Sirbu *et al.,* 2005). Another region of the embryo where *Raldh* and *Cyp26* domains are closely associated is seen in the developing eye (McCaffery *et al.,* 1999).

To begin to assess the function of the *Cyp26* genes their action

Abbreviations used in this paper: BMN, brachial motor neuron; DEAB, 4-diethylaminobenzaldehyde; MO, morpholino oligonucleotide; RA, retinoic acid; RALDH, retinaldehyde dehydrogenase; RAR, retinoic acid receptor.

***Address correspondence to:** Malcolm Maden. MRC Centre for Developmental Neurobiology, 4th floor New Hunt's House, King's College London, Guy's Campus, London Bridge, London SE1 1UL, UK. Fax: +44-207-848-6798. e-mail: malcolm.maden@kcl.ac.uk

0214-6282/2007/$30.00

Printed in Spain
www.intjdevbiol.com

can be prevented either by mutating the gene in mouse or by using antisense morpholino oligonucleotides in other vertebrates. The *Cyp26A1* knockout phenotype in mouse embryos includes sirenomelia, vertebral defects and hindbrain defects (Abu-Abed *et al.,* 2001; Sakai *et al.,* 2001). Sirenomelia is a feature of excessive RA signalling in the tail bud involving the down-regulation of *Wnt3a* and *brachyury* (Sakai *et al.,* 2001) and posterior defects of the hindgut and urogenital system are also a teratological feature of excess RA. Vertebral alterations included missing lumbar, sacral and caudal vertebrae and there was suggestion of anterior to posterior vertebral transformations in the cervical region. Again this defect is suggestive of excessive RA signalling (Kessel & Gruss, 1991). In the hindbrain there was a decreased size of rhombomeres 2 and 3, a larger rhombomere 4 and a possible partial transformation of r2 into a r4-like rhombomere. The latter is a feature of RA excess (Marshall *et al.,* 1992). When the level of RA in the mouse embryo is lowered by generating a *Raldh2*-/+ heterozygote then the posterior truncations in the *Cyp26A1* mutant are rescued in the double mutant, *Raldh2*-/+, *Cyp26A1*-/- (Niederreither *et al.,* 2002). Similarly, in the *Xenopus* embryo over-expression of *Cyp26A1* is able to rescue the effects of exogenous RA treatment (Holleman *et al.,* 1998). These data support the concept that the function of the *Cyp26s* is to switch off the RA signal.

In zebrafish, the *giraffe* mutant has a nonsense mutation in the *Cyp26A1* gene resulting in a truncated protein and the *gir* phenotype is mimicked by the injection of antisense mopholinos to *Cyp26A1* (Emoto *et al.,* 2005). The phenotype is different to that seen in the mouse knockout. In this zebrafish mutant there is a defective common cardinal vein resulting in a failure of blood cell circulation, a failure of fin buds to develop associated with a loss of *Shh* and *Tbx5.1* expression and a reduction in the size of the rostral hindbrain rhombomeres to compensate for an expansion in the rostral spinal cord territory. These phenotypes are not characteristic of RA excess, instead they are reminiscent of RA deficiency: the vitamin A deficient quail fails to form the vitelline vein resulting in a failure of blood cell circulation (Dersch & Zile, 1995); zebrafish embryos treated with citral, a RA synthesis inhibitor, fail to form fins (Vandersea *et al.,* 1998) as does the *Raldh2* mutant zebrafish (Begemann *et al.,* 2001; Grandel *et al.,* 2002); and a reduced hindbrain size is characteristic of the *Raldh2* mutant zebrafish and zebrafish and chick embryos treated with a RA synthesis inhibitor (Begemann *et al.,* 2004) or an inhibitor of RA signalling (Dupe & Lumsden, 2001).

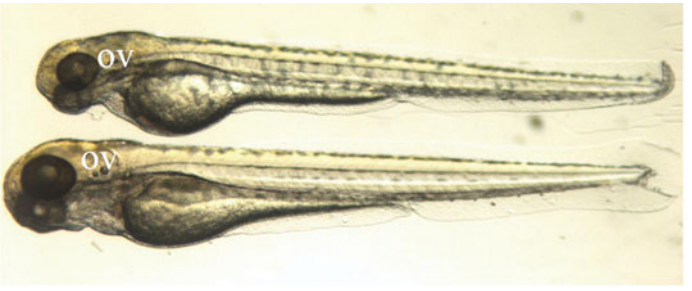

Fig. 2. External appearance of prim-22 (35 hpf) wild-type (lower embryo) and Cyp26B1-splice-MO injected embryos (upper embryo) *revealing that the Cyp26B1-splice-MO injected embryos exhibit a decrease in the size of the head region, smaller otic vesicle (ov) and microphthalmia, whereas the trunk seems very similar to normal.*

The *Cyp26B1* knockout mouse embryo has craniofacial defects including micrognathia which have not yet been described in detail and reduced limbs (Yoshiro *et al.,* 2004). The autopod, zeugopod and stylopod were truncated and fused and in limb bud stages the proximally expressed *Meis* genes were expanded distally due to the distal expansion of RA signalling. This type of limb abnormality is commonly found after excess RA treatment to mammalian embryos (Kochhar, 1973) as is the distal expansion of *Meis* genes (Mercarder *et al.,* 2000).

From the above analysis it seems that the *Cyp26* knockout mouse and zebrafish phenotypes differ in principle: those in the mouse mimic excess RA administration whereas those in the zebrafish resemble a loss of RA signalling. However, only one *Cyp26*-/- phenotype has thus far been reported in the zebrafish, that of *Cyp26A1*, so the available data is rather limited. To this end we describe here the phenotype of a morpholino knockdown of the second *Cyp26* gene, *Cyp26B1*, in zebrafish. We find a phenotype which has some similarities in the hindbrain to the *gir* mutant in that it is smaller, but the major phenotype is a loss of the lower jaw and branchial arch cartilages which have been analysed in detail. We have tried to determine whether this resembles a RA excess or a RA deficiency phenotype by

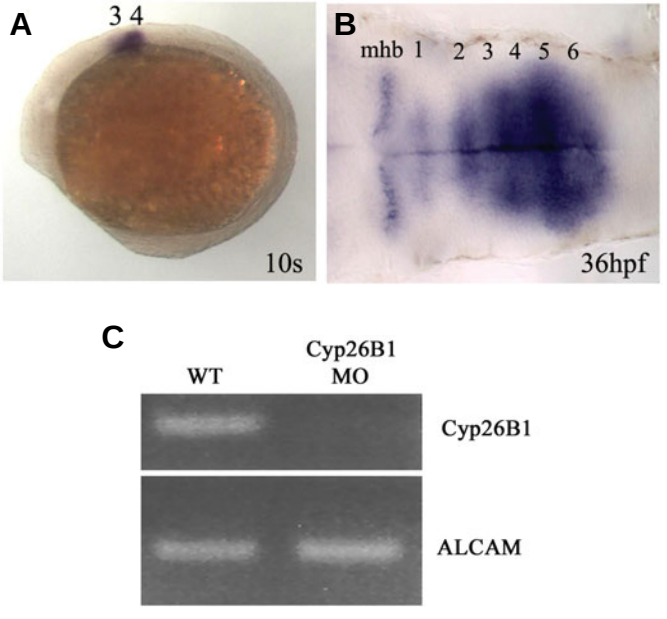

Fig. 1. (A,B) Cyp26B1 expression at two stages of zebrafish development as examples. (A) *Lateral view of a 10 somite stage embryo showing expression in rhombomeres 3 and 4.* **(B)** *Flatmount of a 36 hour hindbrain with extensive Cyp26B1 expression in the rhombomeres. Rhombomere numbers are marked; mhb, midbrain/hindbrain border.* **(C)** *Semi-quantitative PCR experiments on 25 hpf wild-type and Cyp26B1 splice-MO injected embryos. The upper panel shows successful PCR amplification at 32 cycles of the Cyp26B1 transcript in uninjected control embryos (WT, left side) compared to the Cyp26B1-splice-MO injected embryos (right side) where the morpholino blocked amplification across the exon1/exon2 spliced donor sequence and no product was detected. The lower panel shows no change in expression of the control gene, ALCAM, in both samples.*

treating embryos with inhibitors of RA synthesis or excess RA and the results suggest that they are more similar to a RA deficiency phenotype. The same applies to the hindbrain brachiomotor analysis and as a result we suggest that the *Cyp26* genes may be behaving differently in the zebrafish than in the mouse embryo.

Results

The expression pattern of *Cyp26B1* has been described before (Zhao *et al.,* 2005) and will not be repeated here. Dynamic expression is seen in various rhombomeres beginning in presumptive r4 and spreading to r1-6 (Fig. 1A, B), in the ventral diencephalon, at the midbrain/hindbrain border, in the branchial arches, in the eye, pectoral fins and the otic vesicle.

Antisense morpholino injection and RT-PCR

An antisense oligonucleotide designed to bind to the exon 1/exon 2 splice donor sequence was synthesised and injected into embryos at the 1-8 cell stage (0.2 - 1.25 hpf) at different concentrations (between 1 mg/ml - 5 mg/ml) to determine the optimum. Injection at a concentration of 2.75 mg/ml (corresponding to ~ 2nl/injection) appeared to produce a phenotype when examined morphologically.

Semiquantitative PCR experiments were performed to verify that this *Cyp26B1* splice MO was binding to the complementary exon1/exon 2 splice donor sequence and preventing splicing of the *Cyp26B1* primary transcript. If endogenous splicing occurred, a product of 246bp would be observed. If the *Cyp26B1*-splice-MO successfully bound to the splice donor region then a 246bp product would not be observed as the resulting product would be in excess of 1.6kb. Fig. 1C shows the results from PCR experiments performed using cDNA from RNA extracted from 25hpf embryos. The upper bands show successful PCR amplification at 32 cycles of a 246bp product in the untreated WT embryos (left side) and confirms that for the injected samples (right side) the *Cyp26B1*-splice-MO bound to the exon1/exon 2 splice donor sequence and blocked PCR amplification across this sequence. The lower bands show no change in the expression of the control gene, *activated leukocyte cell adhesion molecule (ALCAM)*, in the *Cyp26B1*-splice-MO injected embryos. These PCR experiments were repeated 3 times using 3 separate batches of cDNA synthesized from RNA extracted from 25hpf wild type control and *Cyp26B1* splice MO injected embryos.

External examination of wild-type and Cyp26B1-*splice-MO injected embryos*

Fig. 2 shows a wild-type embryo (lower embryo) and a *Cyp26B1*-splice-MO injected embryo (upper embryo) at matched somite stages. The *Cyp26B1*-splice-MO injected embryos exhibit an overall decrease in size of the head region, smaller otic vesicle and microphthalmia, but from the otic vesicle posterior there was no difference in the length of the embryos. This phenotype was observed in 77% of embryos examined (83 out of 107 embryos). Cardiac oedema was exhibited in a small number of embryos (5%).

Hindbrain gene expression domains and BMN organisation

Because of the smaller size of the head we determined whether there was a hindbrain phenotype, for example missing rhombomeres. In fact all the rhombomeres were present, but they were reduced in size by about 40% in terms of dimensions and cell number. Rhombomere 4, for example, as marked by *Hoxb1A* expression was smaller (Fig. 3A, B), the distance from the midbrain/hindbrain border was shorter (Fig. 3C, D) and the *Krox-20* stripes in r3 and r5 were narrower (Fig. 3E, F). The only

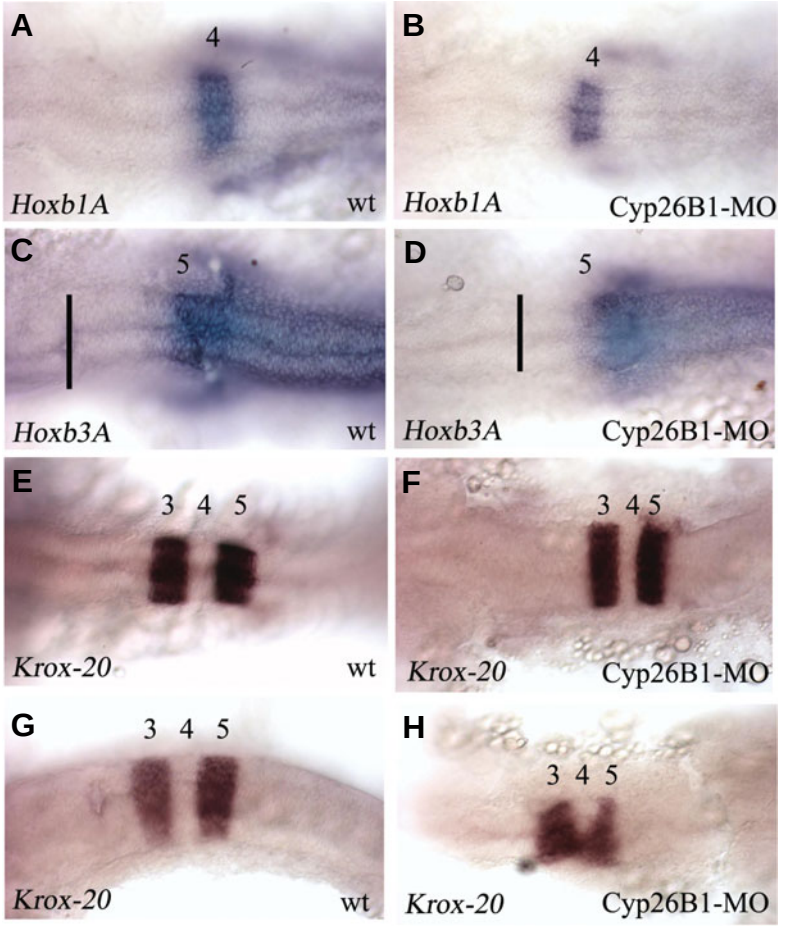

Fig. 3. Expression of three hindbrain genes in control and morpholino injected embryos. (A) *Control* Hoxb1A *expression at the 18 somite stage in rhombomere 4.* **(B)** *Morpholino injected embryo at the 18 somite stage showing normal* Hoxb1A *expression, but r4 is reduced in size.* **(C)** *Control* Hoxb3A *expression at the 18 somite stage showing the distance between the midbrain/hindbrain border (black line) and the expression from r5 caudally.* **(D)** *Morpholino injected embryo at the 18 somite stage showing normal* Hoxb3A *expression, but the distance from the midbrain/hindbrain border (black line) is reduced.* **(E)** *Krox-20 expression in r3 and r5 in a normal 10 somite stage embryo.* **(F)** *Krox-20 expression in a 10 somite stage morpholino injected embryo showing the reduced size of r3 and r5.* **(G)** *Krox-20 expression in r3 and r5 in a normal 18 somite stage embryo.* **(H)** *Krox-20 expression in a morpholino injected 18 somite stage embryo showing ectopic expression into the gap between r3 and r5.*

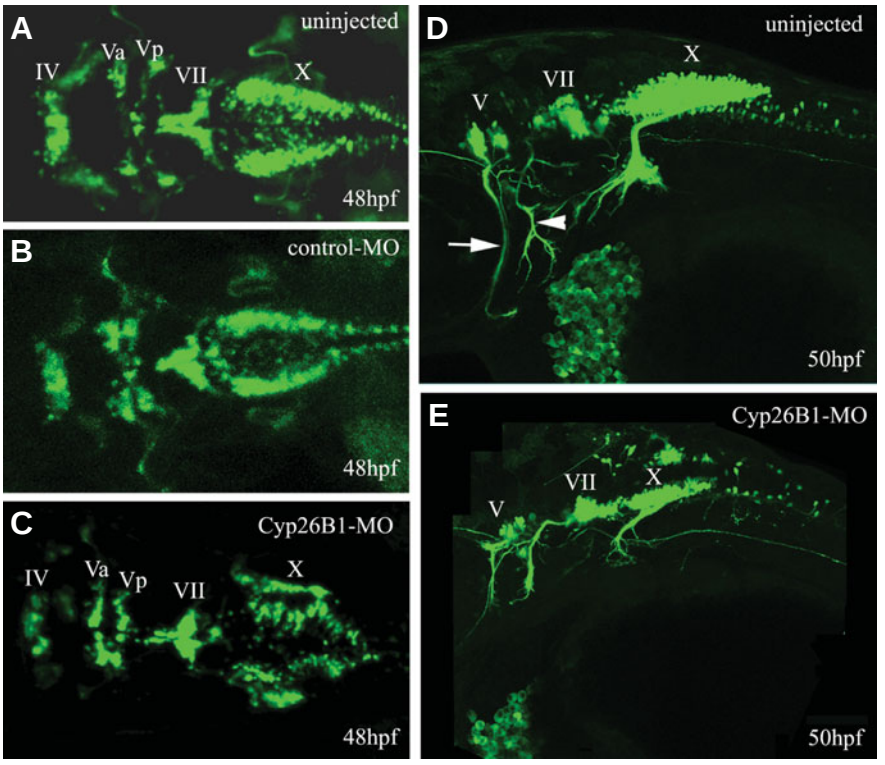

Fig. 4. Confocal micrographs of the brachiomotor neuron (BMN) pattern in the hindbrains of control and morpholino injected embryos examined using the Islet-1-GFP transgenic zebrafish. (A-C) *Dorsal views of the hindbrain, rostral is to the left.* **(D,E)** *Lateral view of the hindbrain; rostral is to the left.* **(A)** *Live, uninjected control embryo at 48 hpf showing neurons of the trochlear nucleus (IV), trigeminal nucleus (Va and Vp), facial nucleus (VII) and the vagal nucleus (nX) which correspond to rhombomeric segmentation.* **(B)** *A hindbrain of a control-MO injected embryo at 48 hpf. The Cyp26B1-splice sequence was scrambled to ensure that any defects exhibited in the hindbrain of the Cyp26B1-splice-MO injected embryos were not due to toxicity problems associated with MO injection. The same organisation of nuclei as seen in (A) is apparent here.* **(C)** *Hindbrain of a Cyp26B1-splice-MO injected embryos at 48 hpf. There is a reduced number of BMNs throughout the smaller hindbrain, but particularly affected is the vagus (X) which shows a strongly reduced number of neurons.* **(D)** *Lateral view of an uninjected control embryo indicating peripherally extending axons from the trigeminal (V) nucleus (white arrow), the facial (VII) nucleus (white arrowhead) and the vagus (X).* **(E)** *Lateral view of a Cyp26B1-splice-MO injected embryo showing much smaller nuclei and far less extensive projections of the axons from those nuclei.*

other abnormality seen in these gene expression patterns was the very occasional loss of the integrity of r4 in that at later stages *Krox-20* expression seemed to be expanding into this rhombomere (Fig. 3H).

To examine the brachial motor neuron (BMN) organisation the *Cyp26B1* MO was injected into embryos carrying the Islet-1-GFP transgene. This transgene is expressed in postmitotic motor neurons early in their development (Higashijima *et al.,* 2000). Injected embryos were stage matched with uninjected controls and the motor neurons examined by confocal microscopy. At 48hpf a control embryo showed a typical organisation of brachimotor neurons with the trochlear nucleus (IV) being the most rostral group, two trigeminal groups (Va and Vp), a characteristic L-shaped facial nucleus (VII) and an extensive cluster of neurons making up the vagus (X) (Fig. 4A). A lateral view of an uninjected control embryo (Fig. 4D) at 50hpf shows peripherally extending axons from the trigeminal (white arrow), facial (white arrowhead) and a large vagus nerve.

A similar organisation of brachiomotor neurons was seen in a control morpholino injected embryo (Fig. 4B). This control was performed to ensure that any motor neuron defects observed in the Cyp26B1-splice-MO injected embryos were not due to toxicity problems associated with MO injection. A morpholino was synthesized that had the splice oligonucleotide sequence scrambled and this was injected into embryos at the same stage and concentration (2.75mg/ml) as the Cyp26B1-splice-MO. Confocal analysis confirmed that the injected control embryos exhibited no motor neuron defects compared to uninjected control embryos (Figs. 4A,B). In contrast, the *Cyp26B1*-splice-MO injected embryos exhibited a decreased overall hindbrain size as expected from the previous *in situ* analysis (Fig. 3). The trochlear, trigeminal and facial nuclei were clearly present in their characteristic locations and with their characteristic shapes, but the most affected structure was the vagus (Fig. 4C) which showed a striking reduction in neuronal number and disorganisation. A lateral view of a 50hpf *Cyp26B1*-splice-MO injected embryo (Fig. 4) revealed that the axonal projections from the trigeminal (nV), facial (nVII) and vagal (nX) neurons were present in their appropriate locations, but their extension and progress was strongly retarded in that they had not innervated the pharyngeal arches. This may suggest an underlying defect in the pharyngeal arches.

Dlx2 *analysis*

In order to begin an analysis of a potential pharyngeal arch problem in these *Cyp26B1*-splice-MO injected embryos we examined the expression of the *Dlx2* gene which is expressed in the migrating neural crest cells populating the visceral arches in zebrafish and mouse (Bulfone *et al.,* 1993; Akimenko *et al.,* 1994) and perturbing this homeobox gene results in cranial cartilaginous defects (Graham, 2002). Treating zebrafish embryos with excess exogenous RA causes a down-regulation of *Dlx2* gene expression resulting in the absence or abnormal development of cranial neural crest-derived cartilaginous elements (Ellies *et al.,* 1997). Therefore, *in situ* hybridisation with a *Dlx2* riboprobe was carried out on 2-day old wild-type and *Cyp26B1*-splice-MO injected embryos to determine whether knocking down the function of *CYP26B1* affected *Dlx2* expression in migrating crest. In control wild-type embryos expression of *Dlx2* was seen in the mandibular pharyngeal arch, the hyoid pharyngeal arch, the second branchial gill arch, the otic vesicle and the pectoral fin (Fig. 5A). *Dlx2* expression was reduced within these domains in *Cyp26B1*-splice-MO injected embryos (Fig. 5B). A ventral view of a wild-type 2 day embryo shows *Dlx2* gene expression in the neural crest cells that will form the components of the lower jaw

(Fig. 5C) whereas in the *Cyp26B1*-splice-MO injected embryos, weaker *Dlx2* expression is observed in this domain (Fig. 5D).

Defective craniofacial cartilage development in the* Cyp26B1-*splice-MO injected embryos

The reduction in *Dlx2* expression and failure of the branchiomotor neurons to extend into the branchial arches suggested the possibility of an arch defect in the absence of *Cyp26B1* expression. To investigate this we cut serial transverse plastic sections of the heads of 35hpf embryos. A section through a normal embryo in Fig. 5E reveals the diencephalon, the layers of the developing retina and lens and the neural crest derived mesenchyme that has formed the craniofacial cartilages such as the trabeculae cranii of the upper jaw and the palatoquadrate and Meckel's cartilage of the lower jaw. Sections though the *Cyp26B1*-splice-MO revealed a complete absence of cartilaginous jaw structures with an almost absent mouth (Fig. 5F). The eyes were smaller in the *Cyp26B1*-splice-MO injected embryos, they were less well differentiated and appeared to have moved ventrally, probably due to the loss of the neural crest derived mesenchyme.

Cartilage staining with Victoria blue was undertaken in 5-day old control and *Cyp26B1* splice-MO injected embryos to more precisely assess the cartilaginous defects. The wild-type viscerocranium is shown in Fig. 6A. Meckel's cartilage and the palatoquadrate are derived from the mandibular pharyngeal arch neural crest, the ceratohyals and the hyosymplectics are derived from the hyoid and posteriorly lie five gill associated ceratobranchial (cb) cartilages, derived from neural crest migrating into pharyangeal arches 3-7. Neural crest migrating into the maxillary process gives rise to the cartilage components of the neurocranium, or upper jaw (Fig. 6B), the trabeculae cranii, ethmoid plate and the posterior parachordal.

Injection of the control MO resulted in no cartilaginous defects (Fig. 6C; 39/39 injected embryos) and the resulting embryos were structurally normal, as they were in terms of their BMN organisation (Fig. 4B). In the *Cyp26B1*-splice-MO injected embryos, on the other hand, the jaw cartilages were severely affected and exhibited a wide range of abnormalities in the upper and/or lower jaw cartilaginous apparatus and/or the gill associated cartilages. An example of the least severely affected embryo is shown in Fig. 6D where only the ceratohyals were affected and instead of projecting rostrally to form the lower jaw they projected medially (Fig. 6D, ch). The ceratohyals, derived from the second arch, were always affected in every embryo and thus seemed to be the most sensitive structure to the loss of *Cyp26B1* expression. The next grade of effect was one in which both the second and first arch derivates were abnormal (Fig. 6E). The ceratohyals projected medio-caudally (Fig. 6E, ch) and the palatoquadrates and Meckel's cartilage were misshapen, the latter forming a more circular structure rather than the characteristic arc and failed to fuse at the midline (Fig. 6E, white arrow). In addition, some of the posterior ceratobranchials, basibranchials and hypobranchials were absent (Fig. 6E, red arrow). In the next most severely affected examples the palatoquadrate cartilages were completely absent (Fig. 6F, white arrow) while Meckel's cartilage was still present and the ceratohyals had their characteristically altered direction of development (Fig. 6F, ch). Most of the ceratobranchials, basibranchials and hypobranchials were absent and this embryo also exhibited cardiac oedema (Fig. 6F, red arrow). An equally affected class of embryo is shown in Fig. 6G where both the

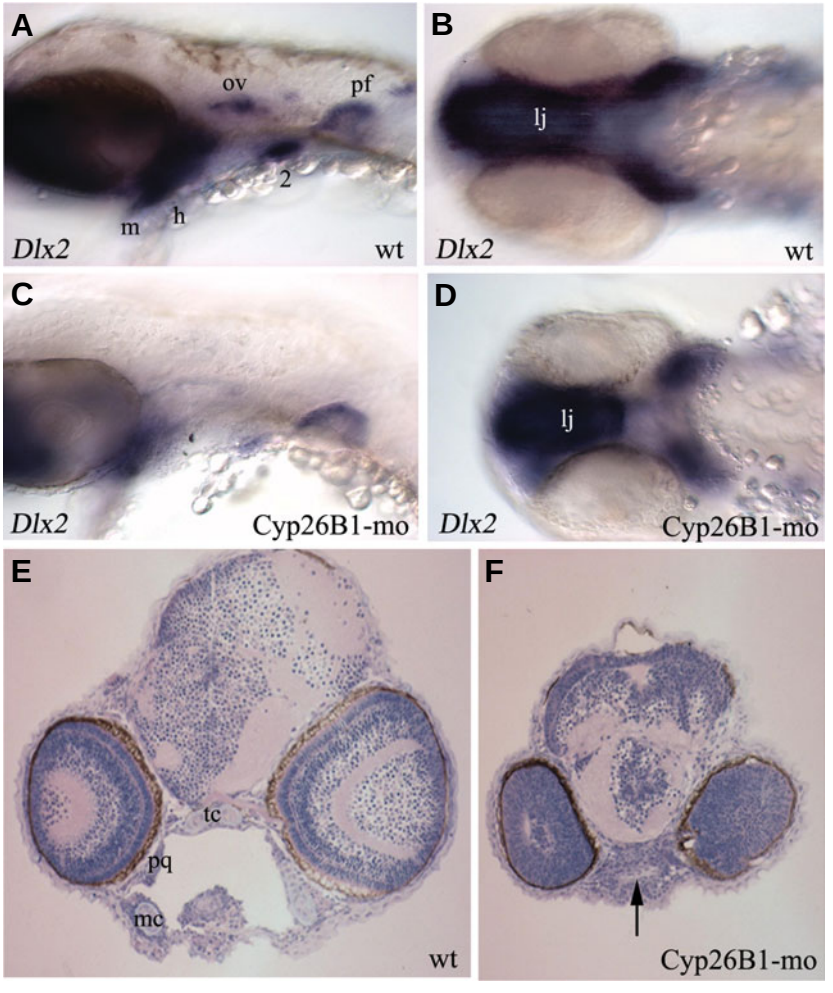

Fig. 5. (A-D) *Dlx2* expression in wild-type and *Cyp26B1*-splice-MO injected embryos. (A) *Lateral view of a wild-type 48 hpf embryo showing* Dlx2 *expression in the 1st mandibular arch (m), the 2nd hyoid arch (h) and branchial gill arch 2 (2), the otic vesicle (ov) and pectoral fins (pf).* **(B)** *Ventral view of a 48 hpf wild-type embryo showing* Dlx2 *expression in the neural crest cells that will form cartilaginous components of the lower jaw (lj).* **(C)** *Lateral view of a* Cyp26B1 *splice MO injected 48 hpf embryo showing strong reduction of* Dlx2 *expression in all the domains except the pectoral fin.* **(D)** *Ventral view of a* Cyp26B1 *splice MO injected 48 hpf embryo showing a reduction of* Dlx2 *expression in the neural crest.* **(E,F)** *Transverse plastic haematoxylin and eosin stained sections of the heads of 35 hpf embryos.* **(E)** *An uninjected control embryo showing the normal structure of the head and cartilaginous components of the jaw. Tc, trabeculae cranii of the upper jaw; pq, palatoquadrate; mc, Meckel's cartilage.* **(F)** *A* Cyp26B1*-splice-MO injected embryo. There is a huge reduction in the size of the head although the brain and eyes are still present. All of the jaw cartilage is absent and there is virtually no mouth (arrow).*

Meckel's and the palatoquadrate cartilages have failed to develop, the certohyals project caudally instead of rostrally and the ceratobranchials on the left side have failed to develop (Fig. 6G, white bracket) which could reflect mosaicism of the splice morpholino. In the most severely affected cases there were no jaw cartilages of the neurocranium or viscerocranium present at all (Fig. 6H) and the eyes moved closer together as shown in the section in Fig. 5F.

In all *Cyp26B1*-splice-MO injected embryos, pectoral fin development appeared normal and the lens always developed despite some embryos exhibiting microphthalmia. A summary of all the cartilaginous jaw/gill structure phenotypes in the *Cyp26B1*-splice-MO injected embryos is presented in Table 1.

DEAB and RA administration

It is clear that injection of the splice MO causes abnormal differentiation in the neural crest derived cartilaginous components of the upper and lower jaw and branchial gill arches 1-5 causing them to be missing or malformed. In an attempt to establish whether the phenotypes observed when preventing translation of *Cyp26B1* might be due to a lack of biologically active CYP26B1 generated RA products, or a failure of CYP26B1 to get rid of the RA signal, thereby exposing embryos to excess RA, embryos were treated with an inhibitor of RA synthesis, 4-diethylaminobenzaldehyde (DEAB), or all-*trans*-RA. Victoria blue preparations were made of 5-day old wild-type embryos treated for 19 hours from 50% epiboly stage (5.3hpf) with separate treatments of 50μM DEAB, 10μM DEAB, 1 x 10^{-8} M all trans RA and 3 x 10^{-9} M all trans RA. As controls, siblings were treated with equivalent concentrations of DMSO, which had no effect.

Treatment with 50μM DEAB resulted in embryos exhibiting many of the cartilaginous phenotypes observed in the *Cyp26B1*-splice-MO injected embryos. The most striking effect was the near complete absence of the neural crest-derived ceratobranchials, basibranchials and hypobranchials from the branchial gill arches 1-5 in 13 out of 14 DEAB treated embryos (Fig. 6I). In 8 out of 14 DEAB treated embryos, the neural crest-derived cartilaginous derivatives of the first arch (Meckel's and the palatoquadrate cartilages) showed a characteristic absence of the palatoquadrates (arrow in Fig. 6J) and a small Meckel's cartilage which did not connect to anything and the characteristic second arch abnormality of medially projecting ceratohyals (Fig. 6J, ch). The similarity between this DEAB treated embryo and the *Cyp26B1* morpholino injected embryo in Fig. 6F is very striking. Components of the second arch (interhyals, ceratohyals and basibranchials) were absent or malformed in 7 out of 14 treated embryos and, as described above, the ceratohyals projected medially instead of rostrally. The neurocranium, although present in all DEAB treated embryos, was misshapen in 3 out of 14 cases. Many of the first and second arch defects present in the morpholino treated embryos were phenocopied by DEAB treatment. For example Fig. 6I shows an embryo with medially projecting ceratohyals with a relatively normal, albeit smaller, Meckel's cartilage and palatoquadrates which is very similar to the mopholino embryo in Fig. 6D.

Very similar results were obtained with 10μm DEAB treated embryos such that the results were indistinguishable. Other abnormalities observed in the DEAB treated embryos at both concentrations were absence of pectoral fins, microphthalmia, cardiac oedema and a reduction in head size.

Treatment with 1 x 10^{-8} M all-*trans*-RA resulted in embryos with a different type of jaw cartilage defect to that seen with DEAB or *Cyp26B1* morpholinos. In 24 out of 24 embryos the cartilaginous derivatives of the first arch (Meckel's cartilage and the palatoquadrate) and the neurocranium were malformed or absent whereas the five gill associated ceratobranchial (cb) cartilages were, in general, well formed (Fig. 6K). This figure shows that as a result of the loss of the neurocranium and the lower jaw the anterior head appeared truncated with the eyes having lost a lot of pigmentation lost their lenses and having come closer together ventrally. The second arch-derived bilateral components of the ceratohyal cartilages were malformed or absent in all 24 out of 24 all-*trans*-RA treated embryos. They did not extend rostrally and appeared thicker, which we interpret as a duplication (Fig. 6K, L ch). Components of the five gill associated branchial arch cartilaginous structures were absent or malformed in only a minority of all-*trans*-RA treated embryos. Other defects observed in the RA treated embryos included duplication of the pectoral fins and cardiac oedema in 100% of cases and microphthalmia or anophthalmia with an absence of the lens.

Treatment with 3 x 10^{-9} M RA resulted in embryos exhibiting many of the phenotypes observed after treatment with 1 x 10^{-8} M all-*trans*-RA, but with less than 100% frequency. The cartilaginous components of the first arch were absent or poorly formed in 24 out of 28 embryos (Fig. 6L) and the neurocranial cartilages were absent or malformed in 22 out of 28 embryos. The second arch-derived ceratohyals were formed and again appeared thickened as if duplicated (as shown in Fig. 6L) in 15 out of 28 all-*trans*-RA treated embryos. Components of the five gill associated branchial arch cartilaginous structures were generally well formed (as shown in Fig. 6K, L) and only reduced or absent in 5 out of 28 embryos. Other defects which appeared were the same as at the higher concentration of RA, but with a reduced frequency including cardiac oedema, duplication of the pectoral fins and only 2 out 28 embryos failed to form a lens.

TABLE 1

ANALYSIS OF CARTILAGINOUS JAW OR GILL MUTANTS AFTER *CYP26B1* MO INJECTION

Phenotypic class	No. of embryos
No phenotype observed	9
Components of the neurocranium missing or malformed	11
Components of mandibular arch missing or malformed	1
Components of hyoid arch missing or malformed	6
Components of mandibular and hyoid arch missing or malformed	16
Components of posterior (gill) arches missing or malformed	31
Components of all pharyngeal arches missing or malformed	9
	(total no. examined 41)

79% of *Cyp26B1*-splice-MO injected embryos exhibited a phenotype

TABLE 2

CARTILAGINOUS JAW OR GILL PHENOTYPES IN THE *CYP26B1*-MORPHOLINO, RA AND DEAB TREATED EMBRYOS

Phenotypic class	*Cyp26B1*-MO	DEAB	RA
Neurocranium absent or malformed	34%	18%	88%
1st and 2nd arches absent or malformed	50%	59%	83.5%
Gill arches absent or malformed	96%	96%	23%

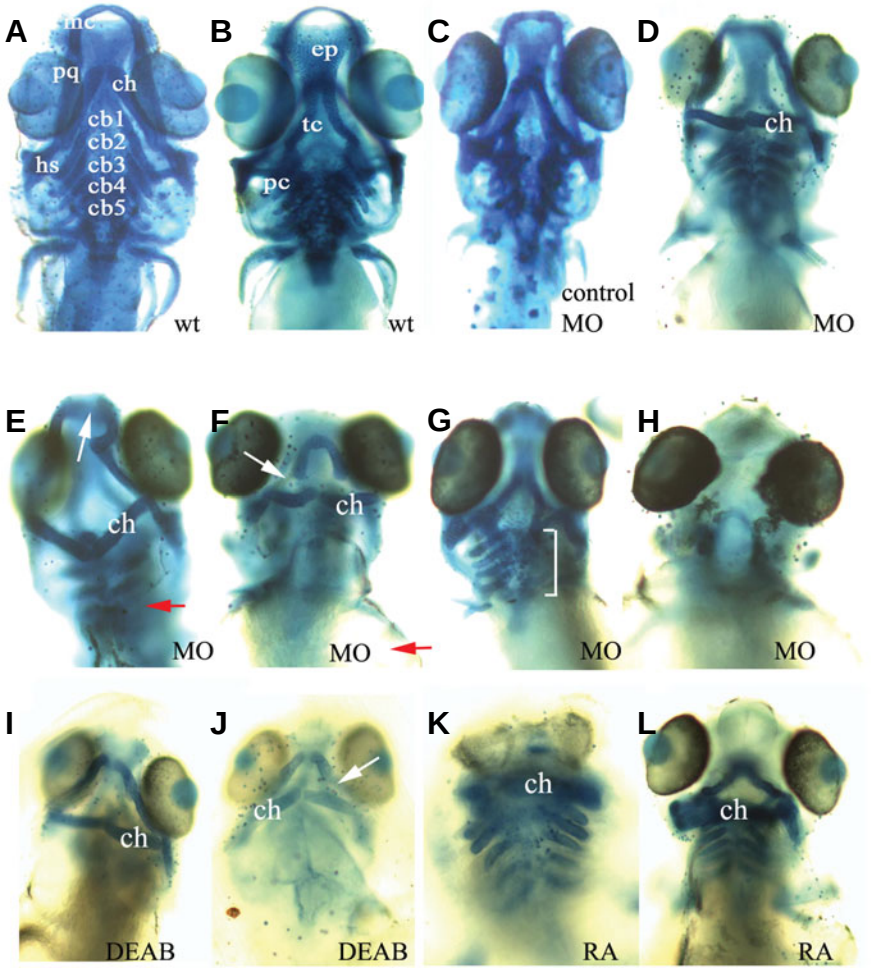

Fig. 6.Ventral views of Victoria blue stained 5-day old embryos to reveal the cartilage. (A,B) *Wild-type;* **(C)** *control MO injected;* **(D-H)** Cyp26B1*-splice-MO injected;* **(I,J)** *DEAB treated;* **(K,L)** *all-trans-RA treated.* **(A)** *Wild-type embryo. Meckel's cartilage (mc) and the palatoquadrate (pq) are formed from the first (mandibular) pharyngeal arch mesenchyme. The supporting ceratohyals (ch) and the hyosympletics (hs) are formed from the second (hyoid) pharyngeal arch mesenchyme. The five gill associated ceratobranchials (cb1-cb5) are formed from the third-seventh pharyngeal arch mesenchyme.* **(B)** *Wild-type embryo showing the neurocranium. The trabeculae cranii (tc), the ethmoid plate (ep) and parachordal cartilage (pc) are formed from neural crest migrating into the frontal nasal process (maxillary).* **(C)** *Control MO injected embryo confirming that cartilaginous defects were not due to the effects of MO toxicity.* **(D)** *The mildest* Cyp26B1*-splice-MO injected phenotype displaying a normal Meckel's cartilage and palatoquadrates, but with ceratohyals (ch) which project medially instead of rostrally.* **(E)** *A more abnormal morpholino phenotype in which Meckel's cartilage is abnormally shaped forming a more circular structure that has failed to meet in the midline (white arrow), the second arch derived ceratohyals (ch) are curving medially and some of the gill associated ceratobranchials are absent (red arrow).* **(F)** *A more abnormal morpholino phenotype where Meckel's cartilage is present, but the palatoquadrates are absent (white arrow), the certaohyals (ch) project medially and all of the gill associated ceratobranchials are absent. This embryo also exhibits cardiac oedema (red arrow).* **(G)** *A severe morpholino phenotype with completely absent first arch components (Meckel's cartilage and palatoquadrates), caudally projecting ceratohyals and the ceratobranchails are missing on one side only (white bracket). The upper jaw of the neurocranium is normal.* **(H)** *The most severe morpholino phenotype with a completely absent jaw apparatus.* **(I)** *DEAB treatment causes a strikingly similar phenotype to the morpholino embryo in (D) with medially projecting ceratohyals (ch).* **(J)** *DEAB treatment has caused a similar phenotype to the morpholino embryo in (F) with missing palatoquadrates (white arrow) and medially projecting ceratohyals (ch).* **(K)** *RA treatment of this embryo has caused an anterior truncation with loss of lenses and pigmentation in the eyes which have moved closed together, missing neurocranium and upper jaw, missing first arch cartilages, thickened certatohyals (ch) which look duplicated and fully present ceratobranchials.* **(L)** *A lower concentration of RA allowed this embryo to develop the upper jaw, but not the first arch components of the lower jaw and, again, the certatohyals (ch) look duplicated.*

A summary of the cartilaginous defects observed in the *Cyp26B1* morpholino embryos in comparison to the RA and DEAB treated embryos is presented in Table. 2.

Discussion

In the work described here we have investigated the role of the CYP26 enzymes in regulating RA signalling by treating zebrafish embryos with a *Cyp26B1* antisense morpholino to determine the effect of knocking down translation of this gene during embryonic development. The developmental abnormalities observed were consistent with the patterns of expression of *Cyp26B1* as there was an overall decrease in the size of the head region with smaller otic vesicles and microphthalmia. The hindbrain, otic vesicle and eye are domains of *Cyp26B1* expression (Zhao *et al.,* 2005).

The reduced head size of morpholino-treated embryos compared to wild-type prompted an analysis of hindbrain gene expression and brachiomotor neuron development. The expression of *Hoxb1A, Hoxb3A* and *Krox-20* was not significantly altered at early stages apart from the clear observation of reduced rhombomere size. There was a suggestion that at later stages the integrity of r4 may break down because we saw an expansion of *Krox-20* expression into r4 in a minority of embryos. This requires a further detailed study.

Using the *Islet-1*-GFP transgenic zebrafish we showed a reduced number of BMNs in the trochlear, trigeminal and facial nuclei, but the greatest effect was on the vagal neurons which were highly disorganised and very reduced in number. *Cyp26B1* is strongly expressed in the posterior hindbrain (Fig. 1B). Perhaps as a result of the reduced neuronal number the axonal projections from the trigeminal, facial and vagal neurons were less prolific and did not appear to extend into the pharyngeal arches which suggested an underlying deficit in pharyngeal arch development. *Cyp26B1* is expressed in the branchial arches (Zhao *et al.,* 2005).

Because of these possible branchial arch defects we examined *Dlx2* expression, a gene which plays an essential role in the

development of craniofacial cartilage as migrating neural crest cells express this gene (Bulfone *et al.,* 1993; Akimenko *et al.,* 1994). Injection of the *Cyp26B1* morpholino resulted in a loss of *Dlx2* expression in the cranial neural crest cells. This led us to examine the jaw cartilage structure of morpholino treated embryos. This revealed that cartilaginous components of the neurocranium were missing or malformed in 34% of the morpholino injected embryos; components of the 1st (mandibular) and 2nd (hyoid) pharyngeal arches were absent or malformed in 50% of morpholino treated embryos; components of the posterior pharyngeal arches 3-7 (branchial – gill – arches 1-5) were missing or malformed in 96% of treated embryos.

We then determined whether this jaw phenotype resembled the effects of excess RA signalling or a deficiency by examining embryos treated with RA or DEAB, the latter being an inhibitor of RA synthesis. After DEAB treatment cartilaginous components of the neurocranium were missing or malformed in 18% of embryos; components of the 1st (mandibular) and 2nd (hyoid) pharyngeal arches were absent or abnormally formed in 59% of embryos; components populating the posterior pharyngeal arches 3-7 were missing or malformed in 96% of DEAB treated embryos. This is a very similar result to that obtained with the morpholino and, furthermore many of the detailed phenotypes of morpholino treatment were mimicked by DEAB. This type of defect where there is a greater prevalence in the more posterior branchial cartilages is seen in the *nls* mutant which has reduced RA signalling caused by a mutation in the *Raldh2* gene (Begemann *et al.,* 2001). On the other hand, excess RA treatment resulted in defective development of cartilage forming the neurocranium in 88% of embryos; components of the 1st and 2nd pharyngeal arches were malformed or missing in 83.5% of RA treated embryos and malformations of the posterior branchial gill arches were observed in 23% of RA treated embryos. Furthermore the most common phenotype we obtained with RA was a duplication of the second arch (certatohyals), the classical response to excess RA (Morriss Kay, 1993), acting via *Hoxa1* (Zhang *et al.,* 1994; Alexandre *et al.,* 1996) and this was never seen after morpholino administration.

So it seemed that these jaw cartilage phenotypes resembled those associated with RA deficiency rather than RA excess and the same conclusion can be arrived at from the effects of the morpholino on BMN organisation. 10^{-8} M RA, administered to *Islet-1*-GFP transgenic zebrafish embryos at late blastula stage resulted in a three-to fourfold increase in vagal BMNs neurons (Linville *et al.,* 2004). In contrast the nls mutant which has reduced RA signalling due to a mutation in the *Raldh2* gene has a vagal nucleus which is reduced by 90% compared to wild type (Begemann *et al.,* 2004). Similarly, when embryos were treated with RA antagonists or DEAB at the blastula stage the same vagal phenotype was observed. Reduced RA signalling on BMNs therefore also accords with the *Cyp26B1* morpholino phenotype. The altered hindbrain structure in which there were no patterning abnormalities, only an overall reduction in size does not resemble the effects of excess RA either. Excess RA results in anterior rhombomere respecification or deletion of the presumptive cerebellar region in zebrafish embryos (Hill *et al.,* 1995).

Recently, Hernandez and colleagues described the hindbrain phenotype resulting from loss of function of *Cyp26a1, Cyp26b1* and *Cyp26c1* in the developing zebrafish embryo (Hernandez *et al.,* 2007). On administering their *Cyp26b1* antisense morpholino they did not observe a phenotype. Their *Cyp26b1* morpholino sequences were based on the ATG region and the exon-2-intron-2 DNA sequences of the *Cyp26b1* gene. We extensively tested three separate morpholino sequences (which were all different from Hernandez and colleagues). Only one of these, the sequence based around the exon-1-intron-1 region of the gene resulted in a phenotype. This may explain why Hernandez *et al.,* did not observe a similar phenotype as observed in this study.

As described in the Introduction there are several aspects of the zebrafish *Cyp26A1* morpholino phenotype which also resemble a lack of RA signalling including loss of pectoral fins and failure of the common cardinal vein to form. Thus although there is solid evidence to support the idea that the CYP26s catabolise the RA signal in the mouse embryo the evidence for a similar role in the zebrafish embryo is by no means so clear cut as the knockdown phenotypes are not the same. It is already known that the products of the CYP26s are biologically active: 4-*oxo*-RA respecifies anteroposterior pattern in the *Xenopus* embryo by activating RARβ (Pijnappel *et al.,* 1993; Nikawa *et al.,* 1995), it can rescue cardiovascular defects in the vitamin A-deficient quail (Kostetskii *et al.,* 1998) and restore sperm production in vitamin A-deficient mice (Gaemers *et al.,* 1996). 4-*oxo*-RA, 4-OH-RA and 5,6-*epoxy*-RA can change epidermal thickness in mouse skin (Reynolds *et al.,* 1993) and each of these compounds can rescue the vitamin A-deficient quail embryo (Reijntjes *et al.,* 2005). Further experiments including rescue of morpholino treated zebrafish with the CYP26 products will provide valuable data on whether these enzymes have different roles in the mouse than in the zebrafish.

Materials and Methods

Zebrafish stocks

Fish lines were maintained at King's College London (KCL). Staging and husbandry was as described by Westerfield (Westerfield, 1995). The transgenic zebrafish embryos expressing green fluorescent protein under the control of the islet-1 promoter were kindly provided by Dr Corinne Houart.

Morpholino synthesis

The mouse CYP26B1 sequence (GenBank accession no. NM_175475) was used to search the zebrafish EST database (www.ensembl.org/Danio_rerio) and these ESTs were used to identify zebrafish contig ctg10569.1 (Sanger Centre assembly 7). The exon splice donor sequences were identified by the consensus sequences around 5' and 3' splice sites – (5')GU and (3')AG of the intron. The nucleotide sequence for exon 1 and the exon 1 splice donor sequence was sent to Gene Tools who identified and synthesized the following oligonucleotide:- CTTACTCGCGCTTAACCTGAAAGAAC. The morpholino was resuspended in sterile H_2O to a concentration of 20 mg/ml and stored at -70ºC.

Embryo microinjection

A morpholino concentration of 2.75 mg/ml was prepared. Approximately 2 nl of morpholino was injected into the yolk of 1-8 cell-stage wild type and islet-1-GFP embryos using a pressurized microinjection device (Picosprizter II, General Value Corporation).

Semiquantitative reverse transcription-PCR

To determine whether the Cyp26B1-splice morpholino was blocking

splicing of the zebrafish Cyp26B1 primary RNA transcripts, semiquantitative reverse transcription-PCR was carried out.

Primer design

The forward primer was selected from exon 1 of ctg20569.1 as follows:-

5'-TGTCCATGGCACTTCTTCTG-3'. The reverse primer was selected from exon 2 of ctg20569.1 as follows:- 5'-ACATTCTCTGCCCCAGTGAC-3'. These nucleotide sequences are complementary to + 814 to +833 (forward) and +1060 to +1041 (reverse) of the Cyp26B1 mRNA (GenBank accession no. AY321366), generating a 246 bp product in wild type zebrafish embryos. Sequences were entered into NCBI BLAST to ensure no sequence homology with known genes.

RNA from 30 somite stage wild type and Cyp26B1 morpholino injected wild type embryos was extracted and measured using the same methods as previously described. For all semiquantitative RT-PCR reactions single-stranded cDNA was synthesised from 1 μg of total cellular RNA. cDNA synthesis was by using M-MuLV reverse transcriptase (Amersham Pharmacia Biotech). The PCR reaction was carried out using 1 μl of the retrotranscription reaction in a final volume of 50 μl, containing 10 x PCR buffer, 1.5 mmol/L $MgCl_2$, 200 μM each dNTPs, 0.2μM each primer and 1.25 units of Taq DNA polymerase (QIAGEN).

The zebrafish ALCAM gene which codes for a cell adhesion molecule (also known as neurogenin) was co-amplified in each experiment to indicate equal amounts of cDNA in the samples and the primers were a kind gift from Dr Chris Mann. Forward and reverse primers were used to generate a 1 kb product. PCR amplification conditions were: 94°C for 3 minutes followed by the cyclic program at 94°C for 30 seconds, 58°C for 30 seconds and 72°C for 1 minute for 32 cycles. For each primer set, an increasing linear number of PCR cycles were performed with otherwise fixed conditions to determine the optimal number of cycles to be used. The PCR products (20 μl) were subjected to electrophoresis in 1% (w/v) agarose gel, visualized by UV after ethidium bromide staining.

Whole mount* in situ *hybridisation

This was performed by standard procedures on dechorionated fixed embryos and involved treatment with Proteinase K, refixing, prehybridisation and a hybridisation mix that contained approximately 1μg/ml DIG labelled antisense RNA probe for Cyp26B1 and hybridisation was carried out overnight at 65ºC. The embryos were washed, blocked with 2% BBR in MABT for 1 hour and incubated overnight in 2% BBR, anti-DIG diluted 1:2000 in MABT at 4ºC. The antibody was removed and the probe detected using BM Purple AP substrate, precipitating (Boehringer Mannheim) and the reaction stopped by washing in 20 mM EDTA in PBST and then the embryos were fixed in 4% PFA.

Victoria blue staining

Embryos were fixed in 4% paraformaldehyde overnight, then placed into 50% ethanol for 15 mins followed by acid alcohol for 1h. They were then stained in 1% Victoria blue (made up in acid alcohol) for 15 mins and dehydrated in a graded series of alcohols (70%, 90%, 95%, 100%, 100%). Finally, the embryos were cleared in methyl salicylate.

Acknowledgements

We would like to thank Carl Hobbs for preparing plastic sections, Corinne Houart for the Islet1-GFP zebrafish embryos and Vicky Prince for zebrafish Hox probes. We also thank the MRC for financial support for this project.

References

ABU-ABED S., DOLLE.P, METZGER D., BECKETT B., CHAMBON P. and PETKOVICH M. (2001). The retinoic acid-metabolizing enzyme, CYP26A1, is essential for normal hindbrain patterning, vertebral identity and development of posterior structures. *Genes Dev.* 15: 226-240.

AKIMENKO M.A., EKKER M., WEGNER J., LIN W. and WESTERFIELD M. (1994). Combinatorial expression of three zebrafish genes related to distal-less: part of a homeobox gene code for the head. *J. Neurosci.* 14: 3475-3486.

ALEXANDRE D., CLARKE J.D.W., OXTOBY E., YAN Y-L., JOWETT T. and HOLDER N. (1996). Ectopic expression of Hoxa-1 in the zebrafish alters the fate of the mandibular arch neural crest and phenocopies a retinoic acid-induced phenotype. *Development* 122: 735-746.

BEGEMANN G., SCHILLING T.F, RAUCH G.J., GEISLER R. and INGHAM P.W. (2001). The zebrafish neckless mutation reveals a requirement for raldh2 in mesodermal signals that pattern the hindbrain. *Development* 128: 3081-3094.

BEGEMANN G., MARX M., MEBUS K., MEYER A. and BASTMEYER M. (2004). Beyond the neckless phenotype: influence of reduced retinoic acid signaling on motor neuron development in the zebrafish hindbrain. *Dev. Biol.* 271: 119-129.

BULFONE A,. KIM H.J., PUELLES L., PORTEUS M.H., GRIPPO J.F. and RUBENSTEIN J.L. (1993). The mouse Dlx-2 (Tes-1) gene is expressed in spatially restricted domains of the forebrain, face and limbs in midgestation mouse embryos. *Mech. Dev.* 40: 129-140.

DE ROOS K., SONNEVELD E., COMPAAN B., TEN BERGE D., DURSTON A.J. and VAN DER SAAG P.T. (1999). Expression of retinoic acid 4-hydroxylase (CYP26) during mouse and Xenopus laevis embryogenesis. *Mech. Dev.* 82: 205-211.

DERSCH H. and ZILE M.H. (1993). Induction of normal cardiovascular development in the vitamin A-deprived quail embryo by natural retinoids. *Dev. Biol.* 160: 424-433.

DUPE V. and LUMSDEN A. (2001). Hindbrain patterning involves graded responses to retinoic acid signalling. *Development* 128: 2199-2208.

ELLIES D.L., LANGILLE R.M., MARTIN C.C., AKIMENKO M.A. and EKKER M. (1997). Specific craniofacial cartilage dysmorphogenesis coincides with a loss of dlx gene expression in retinoic acid-treated zebrafish embryos. *Mech. Dev.* 61: 23-36.

EMOTO Y., WADA H., OKAMOTO H., KUDO A. and IMAI Y. (2005). Retinoic acid-metabolizing enzyme Cyp26a1 is essential for determining territories of hindbrain and spinal cord in zebrafish. *Dev. Biol.* 278: 415-427.

FREEMAN M.(2000). Feedback control of intercellular signalling in development. *Nature* 408: 313-319.

FUJII H., SATO T., KANEKO S., GOTOH O., FUJII-KURIYAMA Y., OSAWA K., KATO S. and HAMADA H. (1997). Metabolic inactivation of retinoic acid by a novel P450 differentially expressed in developing mouse embryos. *EMBO J* 16: 4163-4173.

GAEMERS I.C., VAN PELT A.M.M., VAN DER SAAG P.T. and, DE ROOIJ D.G. (1996). All-trans-4-oxo-retinoic acid: a potent inducer of in vivo proliferation of growth-arrested A spermatogonia in the vitamin A-deficient mouse testis. *Endocrinology* 137: 479-486.

GRAHAM A. (2002). Jaw development: chinless wonders. *Curr. Biol.* 12: R810-R812.

GRANDEL H., LUN K., RAUCH G-J., RHINN M., PIOTROWSKI T., HOUART C., SORDINO P., KUCHLER A.M., SCHULTE-MERKER S., GEISLER R., HOLDER N., WILSON S.W. and BRAND, M. (2002). Retinoic acid signalling in the zebrafish embryo is necessary during pre-segmentation stages to pattern the anterior-posterior axis of the CNS and to induce a pectoral fin bud. *Development* 129: 2851-2865.

GU X., XU F., WANG X., GAO X. and ZHAO Q. (2005). Molecular cloning and expression of a novel CYP26 gene (cyp26d1) during zebrafish early development. *Gene Expr. Patt.* 5: 733-739.

HERNANDEZ R.E., PUTZKE A.P., MYERS J.P., MARGARETHA L. and MOENS C.B. (2007). Cyp26 enzymes generate the retinoic acid response pattern necessary for hindbrain development. *Development* 134: 177-187.

HIGASHIJIMA S., HOTTA Y. and OKAMOTO H. (2000). Visualization of cranial motor neurons in live transgenic zebrafish expressing green fluorescent protein under the control of the islet-1 promoter/enhancer. *J. Neurosci.* 20: 206-218.

HILL J., CLARKE J.D., VARGESSON N., JOWETT T. and HOLDER N. (1995). Exogenous retinoic acid causes specific alterations in the development of the midbrain and hindbrain of the zebrafish embryo including positional respecification of the Mauthner neuron. *Mech. Dev.* 50: 3-16.

HOLLEMANN T., CHEN Y., GRUNZ H. and PIELER T. (1998). Regionalized metabolic activity establishes boundaries of retinoic acid signalling. *EMBO J.*

17: 7361-7372.

KASTNER P., CHAMBON P. and LEID M. 1(994). Role of Nuclear retinoic acid recepotors in the regulation of gene expression. In *Vitamin A in Health and Disease*. pp.189-238. Marcel Dekker, New York.

KESSEL M. and GRUSS P. (1991). Homeotic transformations of murine vertebrae and concomitant alteration of Hox codes induced by retinoic acid. *Cell* 67: 89-104.

KLIEWER S.A., UMESONO K., EVANS R.M. and MANGELSDORF D. (1994). The retinoid X receptors: modulators of multiple hormonal signalling pathways. In *Vitamin A in Health and Disease*. pp. 239-256. Marcel Dekker, New York.

KOCHHAR D.M. (1973). Limb development in mouse embryos. Analysis of teratogenic effects of retinoic acid. *Teratology* 7: 289-298.

KOSTETSKII I., YUAN S-Y., KOSTETSKAIA E., LINASK K.K., BLANCHET S., SELEIRO E., MICHAILLE J-J,. BRICKELL P. and ZILE M. (1998). Initial retinoid requirement for early avian development coincides with retinoid receptor coexpression in the precardiac fields and induction of normal cardiovascular development. *Dev. Dynam.* 213: 188-198.

LINVILLE A., GUMUSANELI E., CHANDRARATNA R.A. and SCHILLING T.F. (2004). Independent roles for retinoic acid in segmentation and neuronal differentiation in the zebrafish hindbrain. *Dev. Biol.* 270: 186-199.

MACLEAN G., ABU-ABED S., DOLLE P., TAHAYATO A., CHAMBON P. and PETKOVICH M. (2001). Cloning of a novel retinoic-acid metabolizing cytochrome P450, Cyp26B1 and comparative expression analysis with Cyp26A1 during early murine development. *Mech. Dev.* 107: 195-201.

MADEN M. 2002. Retinoid signalling in the development of the central nervous system. *Nature Neurosci.* 3: 843-853.

MARSHALL H., NONCHEV S., SHAM M.H., MUCHAMORE I., LUMSDEN A. and KRUMLAUF R. (1992). Retinoic acid alters hindbrain Hox code and induces transformation of rhombomeres 2/3 into a 4/5 identity. *Nature* 360: 737-741.

MCCAFFERY P., WAGNER E., O'NEIL J.O., PETKOVICH M. and DRAGER U.C. (1999). Dorsal and ventral territories defined by retinoic acid synthesis, breakdown and nuclear receptor expression. *Mech. Dev.* 82: 1190130.

MERCADER N., LEONARDO E., PIEDRA M.E., MARTINEZ A.C., ROS M.A. and TORRES M. (2000). Opposing RA and FGF signals control proximodistal vertebrate limb development through regulation of Meis genes. *Development* 127: 3861-3970.

MORRISS-KAY G. (1993). Retinoic acid and craniofacial development: molecules and morphogenesis. *BioEssays* 15: 9-15.

NIEDERREITHER K., ABU-ABED S., SCHUBAUR B., PETKOVICH M., CHAMBON P. and DOLLE P. (2002). Genetic evidence that oxidative derivatives of retinoic acid are not involved in retinoid signalling during mouse development. *Nature Genet.* 31: 84-88.

NIKAWA T., SCHULZ W.A., VAN DEN BRINK C.E., HANUSCH M., VAN DER S.P., STAHL W. and SIES H. (1995). Efficacy of all-trans-beta-carotene, canthaxanthin and all-trans-, 9-cis- and 4-oxoretinoic acids in inducing differentiation of an F9 embryonal carcinoma RAR beta-lacZ reporter cell line. *Arch. Biochem Biophys.* 316: 665-672.

PIJNAPPEL W.W.M., HENDRICKS H.F.J., FOLKERS G.E., VAN DEN BRINK C.E., DEKKER E.J., EDELENBOSCH C., VAN DER SAAG P.T. and DURSTON A.J. (1993). The retinoid ligand 4-oxo-retinoic acid is a highly active modulator of positional specification. *Nature* 366: 340-344.

REIJNTJES S., GALE E. and MADEN M. (2003). Expression of the retinoic acid catabolising enzyme CYP26B1 in the chick embryo and its regulation by retinoic acid. *Gene Expr. Patt.* 3: 621-627.

REIJNTJES S., GALE E and MADEN M. (2004). Generating gradients of retinoic acid in the chick embryo: Cyp26C1 expression and a comparative analysis of the Cyp26 enzymes. *Dev. Dynam.* 230: 509-517.

REIJNTJES S., BLENTIC A., GALE E. and MADEN M. (2005). The control of morphogen signalling: Regulation of the synthesis and catabolism of retinoic acid in the developing embryo. *Dev. Biol.* 285: 224-237.

REYNOLDS N.J., FISHER G.J., GRIFFITHS C.E., TAVAKKOL A., TALWAR H.S., ROWSE P.E., HAMILTON T.A. and VOORHEES J.J. (1993). Retinoic acid metabolites exhibit biological activity in human keratinocytes, mouse melanoma cells and hairless mouse skin in vivo. *J. Pharmacol. Exp. Ther.* 266: 1636-1642.

SAKAI Y., MENO C., FUJII H., NISHINO J., SHIRATORI H., SAIJOH Y., ROSSANT J. and HAMADA H. (2001). The retinoic acid-inactivating enzyme CYP26 is essential for establishing an uneven distribution of retinoic acid along the anterio-posterior axis within the mouse embryo. *Genes Dev.* 15: 213-225.

SIRBU I.O., GRESH L., BARRA J. and DUESTER G. (2005). Shifting boundaries of retinoic acid activity control hindbrain segmental gene expression. *Development* 132: 2611-2622.

SWINDELL E.C., THALLER C., SOCKANATHAN S., PETKOVICH M., JESSELL T.M. and EICHELE G. (1999). Complementary domains of retinoic acid production and degradation in the early chick embryo. *Dev. Biol.* 216: 282-296.

TAHAYATO A., DOLLE P. and PETKOVICH M. (2003). Cyp26C1 encodes a novel retinoic acid-metabolizing enzyme expressed in the hindbrain, inner ear, first branchial arch and tooth buds during murine development. *Gene Exp. Patt.* 3: 449-454.

VANDERSEA M.W., FLEMING P., MCCARTHY R.A. and SMITH D.G. (1998). Fin duplications and deletions induced by disruption of retinoic acid signaling. *Dev. Genes Evol.* 208: 61-68.

WESTERFIELD M. (1995). The zebrafish Book. Guide for the Laboratory Use of Zebrafish (Danio rerio). Univ of Orgeon Press, Eugene.

WHITE J.A., BECKETT-JONES B., GUO Y.D., DILWORTH F.J., BONASORO J., JONES G. and PETKOVICH M. (1997). cDNA cloning of human retinoic acid-metabolizing enzyme (hP450RAI) identifies a novel family of cytochromes P450. *J. Biol. Chem.* 272: 18538-18541.

WHITE J.A., RAMSHAW H., TAIMI M., STANGLE W., ZHANG A, EVERINGHAM S., CREIGHTON S., TAM S.P., JONES G. and PETKOVICH M. (2000). Identification of the human cytochrome P450, P450RAI-2, which is predominantly expressed in the adult cerebellum and is responsible for all-trans-retinoic acid metabolism. *Proc. Natl. Acad. Sci. USA* 97: 6403-6408.

YASHIRO K., ZHAO X., UEHARA M., YAMASHITA K., NISHIJIMA M., NISHINO J., SAIJOH Y., SAKAI Y. and HAMADA H. (2004). Regulation of retinoic acid distribution is required for proximodistal patterning and outgrowth of the developing mouse limb. *Develop. Cell* 6: 411-422.

ZHAO Q., DOBBS-MCAULIFFE B. and LINNEY E. (2005). Expression of cyp26b1 during zebrafish early development. *Gene. Expr. Patt.* 5: 363-369.

ZHANG M., KIM H-J., MARSHALL H., GENDRON-MAGUIRE M., LUCAS D.A., BARON A., GUDAS L.J., GRIDLEY.T, KRUMLAUF R and GRIPPO JF. (1994). Ectopic Hoxa-1 induces rhombomere transformation in mouse hindbrain. *Development* 120: 2431-2442.

Received: 7th December 2006
Reviewed by Referees: 16th March 2007
Modified by Authors and Accepted for Publication: 8th May 2007
Published Online: 25th June 2007

IJDB Special Issue on

THE NOGENT INSTITUTE

Institut d'Embryologie Cellulaire et Moleculaire Nogent-sur-Marne

Edited by Françoise Dieterlen

ORDER BY

Web: http://www.intjdevbiol.com
E-mail: ijdb@ehu.es
FAX: +34-94-601-3266
POST: to the address shown to the right

Price: US$ 90 or Euro €70 per copy (including post and packaging)

The International Journal of Developmental Biology
Editorial Office, Uni. of the Basque Country
Faculty of Medicine, E-48940 Leioa
Vizcaya, SPAIN

UBC Press